

General Disclaimer

One or more of the Following Statements may affect this Document

- This document has been reproduced from the best copy furnished by the organizational source. It is being released in the interest of making available as much information as possible.
- This document may contain data, which exceeds the sheet parameters. It was furnished in this condition by the organizational source and is the best copy available.
- This document may contain tone-on-tone or color graphs, charts and/or pictures, which have been reproduced in black and white.
- This document is paginated as submitted by the original source.
- Portions of this document are not fully legible due to the historical nature of some of the material. However, it is the best reproduction available from the original submission.

Analytical Investigation of the Dynamics
of Tethered Constellations in Earth Orbit (Phase II)

Contract NAS8-36606

Quarterly Report # 1

For the period 22 February 1985 through 21 June 1985

Principal Investigator
Dr. Enrico Lorenzini

Co-Investigator
Mr. David A. Arnold
Dr. Mario D. Grossi
Dr. Gordon E. Gullahorn

July 1985

Prepared for
National Aeronautics and Space Administration
Marshall Space Flight Center, Alabama 35812

Smithsonian Institution
Astrophysical Observatory
Cambridge, Massachusetts 02138

The Smithsonian Astrophysical Observatory
is a member of the
Harvard-Smithsonian Center for Astrophysics

CONTENTS

	Page
SECTION 1.0 INTRODUCTION	4
2.0 TECHNICAL ACTIVITY DURING REPORTING PERIOD AND PROGRAM STATUS	5
2.1 Introductory Remarks	5
2.2 Two-Dimensional Equations Of Motion For A Single-Axis Vertical Constellation With Three Masses	5
2.2.1 General Case	7
2.2.2 Case Of The Middle Mass At The System Center Of Mass . .	13
2.3 Numerical Integration Of The Two-Dimensional Equations Of Motion	15
2.4 Deployment Maneuver	16
2.4.1 Control Laws	16
2.4.2 Simulation Results	18
2.4.3 Concluding Remarks	29
3.0 PROBLEMS ENCOUNTERED DURING REPORTING PERIOD.	29
4.0 ACTIVITY PLANNED FOR THE NEXT REPORTING PERIOD	30

Analytical Investigation of the Dynamics
of Tethered Constellations in Earth Orbit (Phase II)

Contract NAS8-36606

Quarterly Report # 1

For the period 22 February 1985 through 21 June 1985

Principal Investigator

Dr. Enrico Lorenzini

July 1985



Prepared for
National Aeronautics and Space Administration
Marshall Space Flight Center, Alabama 35812

Smithsonian Institution
Astrophysical Observatory
Cambridge, Massachusetts 02138

The Smithsonian Astrophysical Observatory
is a member of the
Harvard-Smithsonian Center for Astrophysics

(NASA-CR-171811) ANALYTICAL INVESTIGATION
OF THE DYNAMICS OF TETHERED CONSTELLATIONS
IN EARTH ORBIT, PHASE 2 Quarterly Report,
22 Feb. - 21 Jul. 1985 (Smithsonian
Institution, Cambridge, Mass.) 31 p

886-13345

886-13345

G3/13 15713

Analytical Investigation of the Dynamics
of Tethered Constellations in Earth Orbit (Phase II)

Contract NAS8-36606

Quarterly Report # 1

For the period 22 February 1985 through 21 June 1985

Principal Investigator
Dr. Enrico Lorenzini

Co-Investigator
Mr. David A. Arnold
Dr. Mario D. Grossi
Dr. Gordon E. Gullahorn

July 1985

Prepared for
National Aeronautics and Space Administration
Marshall Space Flight Center, Alabama 35812

Smithsonian Institution
Astrophysical Observatory
Cambridge, Massachusetts 02138

The Smithsonian Astrophysical Observatory
is a member of the
Harvard-Smithsonian Center for Astrophysics

CONTENTS

	Page
SECTION 1.0 INTRODUCTION	4
2.0 TECHNICAL ACTIVITY DURING REPORTING PERIOD AND PROGRAM STATUS	5
2.1 Introductory Remarks	5
2.2 Two-Dimensional Equations Of Motion For A Single-Axis Vertical Constellation With Three Masses	5
2.2.1 General Case	7
2.2.2 Case Of The Middle Mass At The System Center Of Mass . .	13
2.3 Numerical Integration Of The Two-Dimensional Equations Of Motion	15
2.4 Deployment Maneuver	16
2.4.1 Control Laws	16
2.4.2 Simulation Results	18
2.4.3 Concluding Remarks	29
3.0 PROBLEMS ENCOUNTERED DURING REPORTING PERIOD.	29
4.0 ACTIVITY PLANNED FOR THE NEXT REPORTING PERIOD	30

Abstract

This Quarterly Report deals with the deployment maneuver of a single-axis, vertical constellation with three masses. A new, easy to handle, computer code that simulates the two-dimensional dynamics of the constellation has been implemented. This computer code is used for designing control laws for the deployment maneuver that minimizes the acceleration level of the low-g platform during the maneuver.

1.0 INTRODUCTION

This is the first Quarterly Report submitted by SAO under contract NAS8-36606, "Analytical Investigation of the Dynamics of Tethered Constellations in Earth Orbit (Phase II)," Dr. Enrico Lorenzini, PI, and covers the period from 22 February 1985 through 21 June 1985.

2.0 TECHNICAL ACTIVITY DURING REPORTING PERIOD AND PROGRAM STATUS

2.1 Introductory Remarks

The results of the study performed under NASA contract NAS8-35497 on the dynamics of tethered constellations in earth orbit were very encouraging for a single-axis vertical constellation. In the three-mass configuration the middle mass, if appropriately placed at the orbital center of the system, can be conveniently utilized as a low-g experiment platform. A preliminary estimation of the acceleration level achievable was around 10^{-8} g when the system began its station-keeping phase from a rest condition and the J_2 term of the gravity field was taken into account. The above referenced report dealt with the station-keeping of the constellation only. No indications were provided on how to deploy the system to the final, steady state configuration. This Quarterly Report addresses problems related to deployment of a single-axis constellation with three masses from the initial, compact configuration to the final alignment of the constellation with the local vertical at fully deployed tether length.

2.2 Two-Dimensional Equations Of Motion For A Single-Axis Vertical Constellation With Three Masses

The SKYHOOK program was used to simulate the station-keeping phase of the constellation in Phase I studies. Station-keeping is easier to model than deployment so that a limited number of simulation runs were required. Deployment of a three-mass constellation is a new topic that requires a longer and more difficult effort. A complex computer code, like SKYHOOK, is therefore prohibitively cumbersome for a parametric study like this. For this reason a more

flexible and easy to handle mathematical model has been derived to study the deployment dynamics of a single-axis constellation with three masses.

The model is two-dimensional. This provides a good approximation of the deployment maneuver that is dominated by forces acting in the plane of the orbit. The model assumes three point masses generically located in space (on the orbital plane) connected by two massless tethers of known elastic characteristics.

The center of mass of the system is supposed to be on a circular or nearly circular orbit but in any case the orbital motion is decoupled by the system oscillation. Presently no aerodynamic forces are in the model but they could be added easily. Aerodynamic forces, however, are not so important during deployment at 500 km altitude. Excessive complication of the model would be impractical since this model is developed in order to design a suitable deployment strategy for verification by SKYHOOK.

The equations of motion were derived by using the Lagrangian formulation. The Lagrangian coordinates were chosen, as shown in Figure (2.2.1), to give an immediate representation of the system oscillations. They also have the advantage of representing oscillatory modes that are, in some cases, very weakly coupled and therefore suitable for consistent simplifications in order to achieve analytical results.

2.2.1 General Case -

The three masses are generically located on the plane of the orbit. With reference to Figure (2.2.1), the position of the masses with respect to a reference frame centered at the center of mass and co-rotating with the system is given by:

$$x_1 = (R_3 \ell_3 - R_1 \ell_1 + \ell_1) \sin \theta - R_2 \epsilon \cos \theta$$

$$x_2 = (R_3 \ell_3 - R_1 \ell_1) \sin \theta + (R_1 + R_3) \epsilon \cos \theta$$

$$x_3 = (R_3 \ell_3 - R_1 \ell_1 - \ell_3) \sin \theta + R_2 \epsilon \cos \theta$$

$$z_1 = (R_3 \ell_3 - R_1 \ell_1 + \ell_1) \cos \theta + R_2 \epsilon \sin \theta$$

$$z_2 = (R_3 \ell_3 - R_1 \ell_1) \cos \theta - (R_1 + R_3) \epsilon \sin \theta$$

$$z_3 = (R_3 \ell_3 - R_1 \ell_1 - \ell_3) \cos \theta + R_2 \epsilon \sin \theta \quad (2.2.1)$$

where:

$$R_i = m_i / m_{\text{tot}} \quad i = 1, 2, 3$$

Equations (2.2.1) are valid for $\epsilon \ll \ell_1$, which is applicable in most cases.

The potential energy of the system is given by:

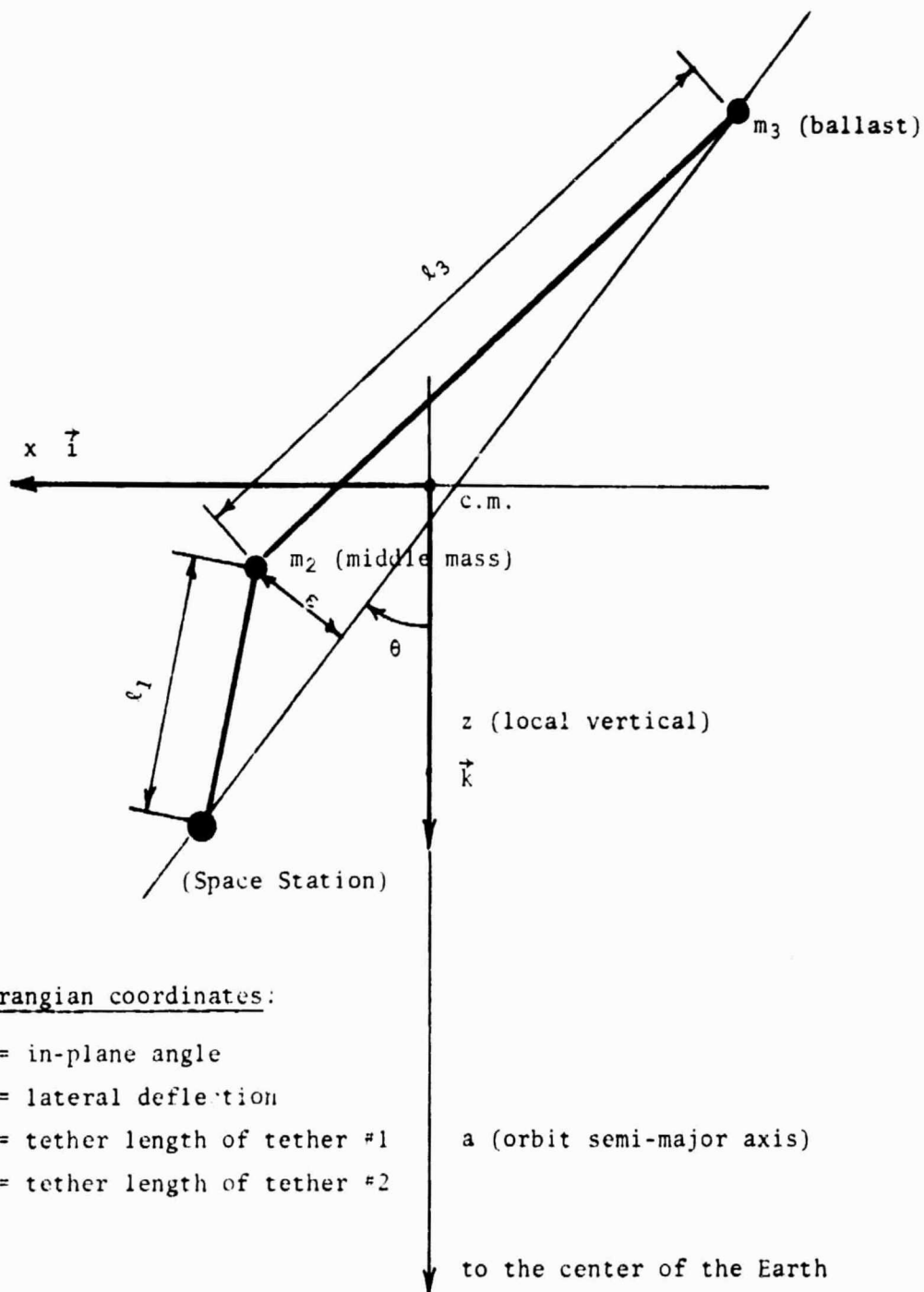


Figure 2.2.1 Geometry and reference frame for a single-axis tethered constellation with three masses.

$$V = \mu \sum_1^3 m_i / r_i \quad (2.2.2)$$

which to the second order of approximation is as follows:

$$V = - \frac{\mu}{a} \sum_1^3 m_i \left[1 + \frac{z_i^2}{a} - \frac{z_i^2 + x_i^2 - 3z_i}{2a^2} \right] \quad (2.2.3)$$

where μ is the gravitational constant of the earth and a is the semi-major axis of the orbit of the system center of mass. After considerable rearranging, the potential energy can be expressed as:

$$\begin{aligned} V = & - \frac{1}{2} \Omega^2 \left\{ m_{\text{tot}} [2a^2 - 2(R_3 \ell_3 - R_1 \ell_1)^2 (3 \cos^2 \theta - 1)] + \right. \\ & + R_2 (m_1 + m_3) [\epsilon^2 (3 \sin^2 \theta - 1)] + \\ & + m_1 \left[\ell_1^2 (3 \cos^2 \theta - 1) + 6 \ell_1 R_2 \epsilon \cos \theta \sin \theta \right] + \\ & \left. + m_3 \left[\ell_3^2 (3 \cos^2 \theta - 1) - 6 \ell_3 R_2 \epsilon \cos \theta \sin \theta \right] \right\} \quad (2.2.4) \end{aligned}$$

where Ω is the mean orbital rate.

The kinetic energy of the system is given by:

$$T = \frac{1}{2} \sum_1^3 m_i |v_i|^2 \quad (2.2.5)$$

where:

$$|v_i|^2 = [\dot{x}_i + \Omega (a - z_i)]^2 + [\dot{z}_i + \Omega x_i]^2 \quad (2.2.6)$$

After taking the derivative of equations (2.2.1) and substituting them into equations (2.2.6) and (2.2.5) we finally get:

$$\begin{aligned}
 T = \frac{1}{2} \left\{ m_{\text{tot}} [\Omega^2 a^2 - (R_2 \ell_2 - R_1 \ell_1)^2 - (R_3 \ell_3 - R_1 \ell_1)^2 (\theta - \Omega)^2] + \right. \\
 + R_2 (m_1 + m_2) [\dot{\epsilon}^2 + \Omega^2 \epsilon^2 + \epsilon^2 (\theta - \Omega)^2] + \\
 + m_1 [\dot{\ell}_1^2 + \ell_1^2 (\theta - \Omega)^2 - 2\Omega R_2 (\ell_1 \dot{\epsilon} - \ell_1 \dot{\theta})] + \\
 \left. + m_3 [\dot{\ell}_3^2 + \ell_3^2 (\theta - \Omega)^2 + 2\Omega R_2 (\ell_3 \dot{\epsilon} - \ell_3 \dot{\theta})] \right\} \quad (2.2.7)
 \end{aligned}$$

The Lagrangian function is easily computed as:

$$L = T - V \quad (2.2.8)$$

The equations of motion are given by:

$$\frac{d}{dt} \left(\frac{\partial L}{\partial \dot{q}_1} \right) - \frac{\partial L}{\partial q_1} = Q_1 \quad (2.2.9)$$

where the Lagrangian coordinates are:

$$q_1 = \theta; \quad q_2 = \epsilon; \quad q_3 = \ell_1; \quad q_4 = \ell_3 \quad (2.2.10)$$

The Q_i 's are the generalized forces given by:

$$Q_j = \sum_1^j \vec{F}_1 \cdot \frac{\partial \vec{F}_1}{\partial q_j} \quad (2.2.11)$$

In equation (2.2.11) \vec{F}_1 are the forces acting on the masses and \vec{r}_1 the radius

vectors, respectively given by:

$$\bar{r}_1 = x_1 \bar{i} + z_1 \bar{k} \quad (2.2.12)$$

$$\bar{F}_1 = -T_1(\cos \theta + \epsilon/l_1 \sin \theta) \bar{k} - T_1(\sin \theta - \epsilon/l_1 \cos \theta) \bar{i}$$

$$\bar{F}_2 = [(T_1 - T_3) \cos \theta + (T_1/l_1 + T_3/l_3) \epsilon \sin \theta] \bar{k} + [(T_1 - T_3) \sin \theta - (T_1/l_1 + T_3/l_3) \epsilon \cos \theta] \bar{i}$$

$$\bar{F}_3 = T_3(\cos \theta - \epsilon/l_3 \sin \theta) \bar{k} + T_3(\sin \theta + \epsilon/l_3 \cos \theta) \bar{i} \quad (2.2.13)$$

By substituting (2.2.12) and (2.2.13) into (2.2.11) we finally get the generalized forces as follows:

$$\begin{aligned} Q_\theta &= 0 \\ Q_\epsilon &= -\epsilon(T_1/l_1 + T_3/l_3) \\ Q_{l_1} &= -T_1 \\ Q_{l_3} &= -T_3 \end{aligned} \quad (2.2.14)$$

where T_1 and T_3 are the tensions in the respective tethers.

By substituting the above into the Lagrangian equations (2.2.9) and after performing the necessary derivations we finally get the equations of motion as follows:

$$\begin{aligned} m_1 \left\{ \delta \left[l_1^2 + l_1(R_3 l_3 - R_1 l_1) \right] + 2l_1(\dot{\theta} - \Omega) [l_1 + (R_3 l_3 - R_1 l_1)] + \right. \\ \left. + 3\Omega^2 l_1 \cos \theta \sin \theta [l_1 + 2(R_3 l_3 - R_1 l_1)] - 3\Omega^2 l_1 R_3 \epsilon \cos(2\theta) \right\} + \end{aligned}$$

$$\begin{aligned}
& + m_3 \left\{ \ddot{\theta} [\ell_3^2 - \ell_3 (R_3 \ell_3 - R_1 \ell_1)] + 2 \ell_3 (\dot{\theta} - \Omega) [\ell_3 + (R_3 \ell_3 - R_1 \ell_1)] + \right. \\
& \quad \left. + 3 \Omega^2 \ell_3 \cos \theta \sin \theta [\ell_3 + 2 (R_3 \ell_3 - R_1 \ell_1)] + 3 \Omega^2 \ell_3 R_2 \epsilon \cos (2\theta) \right\} + \\
& \quad + R_2 (m_1 + m_3) [\epsilon^2 \ddot{\theta} + 2 \epsilon \dot{\epsilon} (\dot{\theta} - \Omega) - 3 \Omega^2 \epsilon^2 \cos \theta \sin \theta] = 0
\end{aligned}$$

$$\begin{aligned}
& R_2 (m_1 + m_3) [\ddot{\epsilon} - \epsilon (\dot{\theta} - \Omega)^2 - 3 \Omega^2 \epsilon \sin^2 \theta] + \\
& + R_2 m_{tot} [3 \Omega^2 \cos \theta \sin \theta (R_3 \ell_3 - R_1 \ell_1) - 2 \Omega (R_3 \dot{\ell}_3 - R_1 \dot{\ell}_1)] = -\epsilon (T_1 / \ell_1 + T_3 / \ell_3) \quad (2.2.15)
\end{aligned}$$

$$\begin{aligned}
& m_1 \left\{ \ddot{\ell}_1 + (R_3 \ddot{\ell}_3 - R_1 \ddot{\ell}_1) - \Omega^2 (3 \cos^2 \theta - 1) [\ell_1 + 2 (R_3 \ell_3 - R_1 \ell_1)] - \right. \\
& \quad \left. - (\dot{\theta} - \Omega)^2 [\ell_1 + (R_3 \ell_3 - R_1 \ell_1)] - 3 \Omega^2 R_2 \epsilon \cos \theta \sin \theta - 2 \Omega R_2 \dot{\epsilon} \right\} = -T_1
\end{aligned}$$

$$\begin{aligned}
& m_3 \left\{ \ddot{\ell}_3 - (R_3 \ddot{\ell}_3 - R_1 \ddot{\ell}_1) - \Omega^2 (3 \cos^2 \theta - 1) [\ell_3 - 2 (R_3 \ell_3 - R_1 \ell_1)] - \right. \\
& \quad \left. - (\dot{\theta} - \Omega)^2 [\ell_3 + (R_3 \ell_3 - R_1 \ell_1)] + 3 \Omega^2 R_2 \epsilon \cos \theta \sin \theta + 2 \Omega R_2 \dot{\epsilon} \right\} = -T_3
\end{aligned}$$

These equations of motion will be used to simulate the dynamics of the three-mass system during deployment as will be shown later in this report. After further simplifications, relevant to particular cases, these equations can also provide information on the dynamics of the system without being numerically integrated.

2.2.2 Case Of The Middle Mass At The System Center Of Mass -

In equations (2.2.15) the term $R_3 \ell_3 - R_1 \ell_1$ is the distance (along the line connecting m_1 and m_3) of the middle mass m_2 from the system center of mass. If the middle mass is maintained constantly at the center of mass by means of an appropriate control law then the above mentioned term and its derivatives can be eliminated in equation (2.2.15). The distances ℓ_1 and ℓ_3 can also be expressed as a function of the overall tether length ℓ . From equation (2.2.13), by requiring that the component of \vec{F}_2 along the line connecting m_1 and m_3 is zero, we get $T_1 = T_3 = T$ so that equations (2.2.15) reduce to:

$$m_{\text{eq}} [\ell^2 \ddot{\theta} + 2\ell \dot{\ell} (\dot{\theta} - \Omega)^2 + 3\Omega^2 \ell^2 \cos \theta \sin \theta] + \\ + R_2 (m_1 + m_3) [\epsilon^2 \ddot{\theta} + 2\epsilon \dot{\epsilon} (\dot{\theta} - \Omega) - 3\Omega^2 \epsilon^2 \cos \theta \sin \theta] = 0$$

$$R_2 [\ddot{\epsilon} - \epsilon (\dot{\theta} - \Omega)^2 - 3\Omega^2 \epsilon \sin^2 \theta] = -\epsilon T / (\ell m_{\text{eq}}) \quad (2.2.16)$$

$$m_{\text{eq}} [\ddot{\ell} - \Omega^2 \ell (3 \cos^2 \theta - 1) - (\dot{\theta} - \Omega)^2 \ell] - \\ - R_2 (m_1 - m_3) [3\Omega^2 \epsilon \cos \theta \sin \theta + 2\Omega \dot{\epsilon}] = -T / m_{\text{eq}}$$

Equations (2.2.16) provide some useful information on the dynamics of the system. The coupling among the rotational motion (equation in θ) and the lateral deflection (equation in ϵ) is strongly reduced by placing the middle mass m_2 at the system center of mass. In particular if the initial lateral displacement is zero it stays zero in spite of the system libration. This suggests, for example, that the best way to deploy the constellation without overly perturbing the low-g platform is to design a control law that keeps the middle mass at the system center of mass throughout the entire deployment. At the end of the

maneuver the mass m_2 can be moved to the orbital center (a few meters below the c.m.) in order to minimize the vertical acceleration.

If we assume that the constellation is fully deployed, that θ and $\dot{\theta}$ are equal to zero so that the tension is approximately constant and is given by $T = 3m_{eq}\Omega^2\ell$, then the ϵ equation in (2.2.16) reduces to:

$$R_2\ddot{\epsilon} + \Omega^2\epsilon(3 - R_2) = 0 \quad (2.2.17)$$

From this extremely simple equation we can derive an analytic formula to compute the free oscillation frequency of the lateral vibration of mass m_2 as follows:

$$f_\epsilon = \frac{1}{2\pi} (3/R_2 - 1)^{1/2}\Omega \quad (2.2.18)$$

As an example, for the constellation studied in Phase I, with: $m_1 = 90600$. kg, $m_2 = 4530$ kg, $m_3 = 9060$. kg, $\Omega = 1.1068 \times 10^{-3}$ rad/sec (altitude = 500 km) we get:

$$f_\epsilon = 1.45 \text{ hz} ; T_\epsilon = 688.4 \text{ sec} \quad (2.2.19)$$

Notice also that in the first approximation the lateral oscillation frequency does not depend on the overall system length. This is because the tension is directly proportional to ℓ while the angle between the tethers and the line through the end masses m_1 and m_3 is inversely proportional to it. The tether length, therefore, cancels out when computing the horizontal component of the force acting upon the middle mass.

2.3 Numerical Integration Of The Two-Dimensional Equations Of Motion

A new software code called 3MASS has been implemented to simulate the dynamics of a 3-mass constellation by using the equations of motion previously described. The computer program uses a fourth order Runge-Kutta integration subroutine with variable step size. This integration has been successfully tested in the past with a similar mathematical model. Additional subroutines called DEPLOY3 and STAKE3 model the tether control laws during the deployment and the station-keeping maneuver respectively. All the geometrical and mass properties and orbital characteristics of the constellation are read as input parameters by the main program and passed to the integrator. The integration subroutine, called DRKGS, calls the subroutine FCT which computes the derivatives of the Lagrangian coordinates. DEPLOY3 or STAKE3 are called by FCT and after a successful integration step the output subroutine OUTF is called. OUTF formats the output variables for the printout and it prepares the output file for the plotter. Subroutine OUTF also stops the program in the case of program malfunctions or the achievement of the desired final conditions.

Typical program malfunctions are: the in-plane angle is too large so that the constellation attitude is close to the horizontal plane or the integration step size becomes too small. This computer program is very efficient, at least when the tethers are considered unstretchable. Normal maximum integration step sizes are around 50 sec. These characteristics make it suitable for deriving appropriate tether control laws for the deployment phase.

2.4 Deployment Maneuver

2.4.1 Control Laws -

Deriving a deployment control law depends on the control parameters available to the deployer and on the measurement accuracy of these parameters. Knowledge of the in-plane and out-of-plane angular rate of the tether libration is required for a very effective damping of librations. Simpler control laws rely on the tether length and length rate or on length, length rate and tension. They are respectively called rate control laws and tension control laws even if the latter denomination is inaccurate. Rate control laws are easy to implement and are very reliable. However, they do not damp librations: the decrease of the libration amplitudes in this case is due to the conservation of angular momentum while the tether length is being varied. The tether tension is, on the contrary, related to libration angles and angular rates (well coupled to the in-plane oscillation and very weakly to the out-of-plane) so that a tension control law, if appropriately tuned to the tether longitudinal oscillation, provides a good damping of the in-plane oscillation. A major drawback is that the tension for short tether lengths is too low to be a reliable parameter to control. For this reason rate control laws (with or without angular feedback) have to be used for short tether lengths. In this study we used a rate control law for deployment mainly for two reasons: a) if low level acceleration can be achieved in the middle mass, notwithstanding a residual oscillation of the system, then any other control law will be more effective than this control law; b) a rate control law constitutes the base for any other more refined control law.

The system starts with the three masses very close together, though not coincident, orbiting in relative equilibrium. The lower mass, m_1 , is the space station, the central mass, m_2 , is the low gravity facility, and the higher mass,

m_3 , is a ballast mass. Thereafter the natural length of each of the two tethers is derived from a control law:

$$\dot{l} = \begin{cases} \alpha l & l_I < l < l_T \\ -\beta(l - l_\sigma) & l_T < l < l_{SK} \end{cases} \quad (2.4.1)$$

where the various parameters may be different for the two tethers. Here l is the deployed natural length, l_I an initial length, l_T a transition length at which the reel begins decelerating, l_{SK} the desired final length, and $l_\sigma = l_{SK} + \sigma$ is the length which would result at infinite time, σ being a small length chosen so that the deployment takes finite time but the cutoff is not too abrupt. The constant $\alpha = 0.75 \Omega \sin(2\theta_c)$ is chosen by analogy to a single mass deployment where it would result in an attitude angle during deployment equal to θ_c ; and $\beta = \alpha l_T / (l_\sigma - l_T)$ is such that the deployment velocity is continuous through the transition. This control law may be solved explicitly to give the deployed natural length as a function of time. Assuming the initial time is $t = 0$, we get

$$l(t) = \begin{cases} l_I e^{\alpha t} & 0 < t < t_T \\ l_\sigma - (l_\sigma - l_T) \exp[-\beta(t - t_T)] & t_T < t < t_{SK} \end{cases} \quad (2.4.2)$$

where $t_T = (1/\alpha) \ln(l_T/l_I)$ is the transition time and $t_{SK} = t_T + (1/\beta) \ln[(l_\sigma - l_T)/\sigma]$ is the turn off time.

The same time constant ($t_{ca} = 1/\alpha$) is used for the two tethers in order to keep the middle mass at the same location throughout the maneuver. The same consideration applies to the time constant for the deceleration phase ($t_{c\beta} = 1/\beta$).

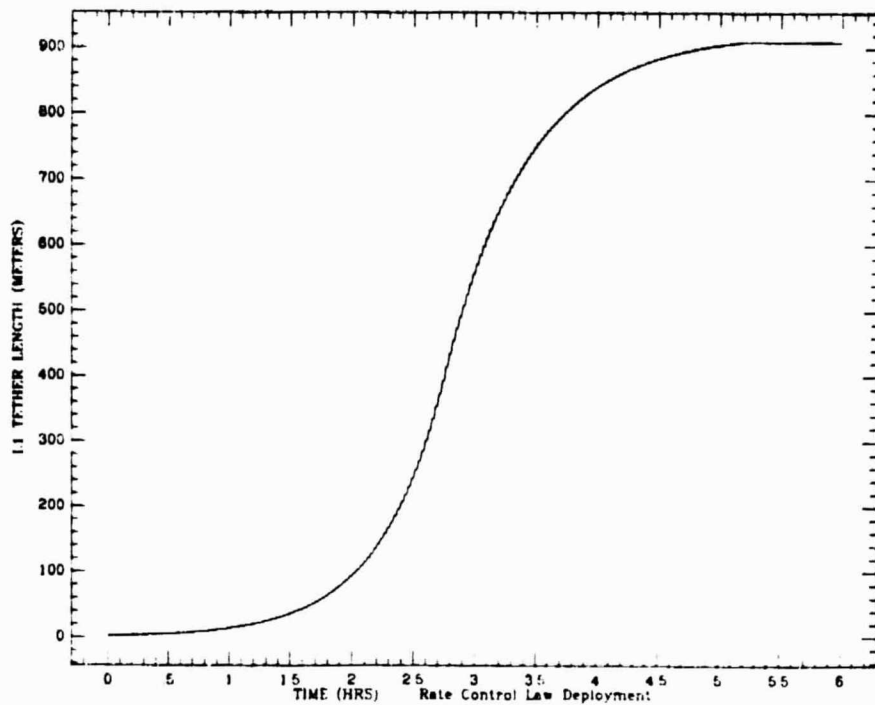
All the characteristic lengths, such as l_T , l_L , σ are in the ratio l_{SK1}/l_{SK3} in order to provide simultaneous transitions in the two tethers.

2.4.2 Simulation Results -

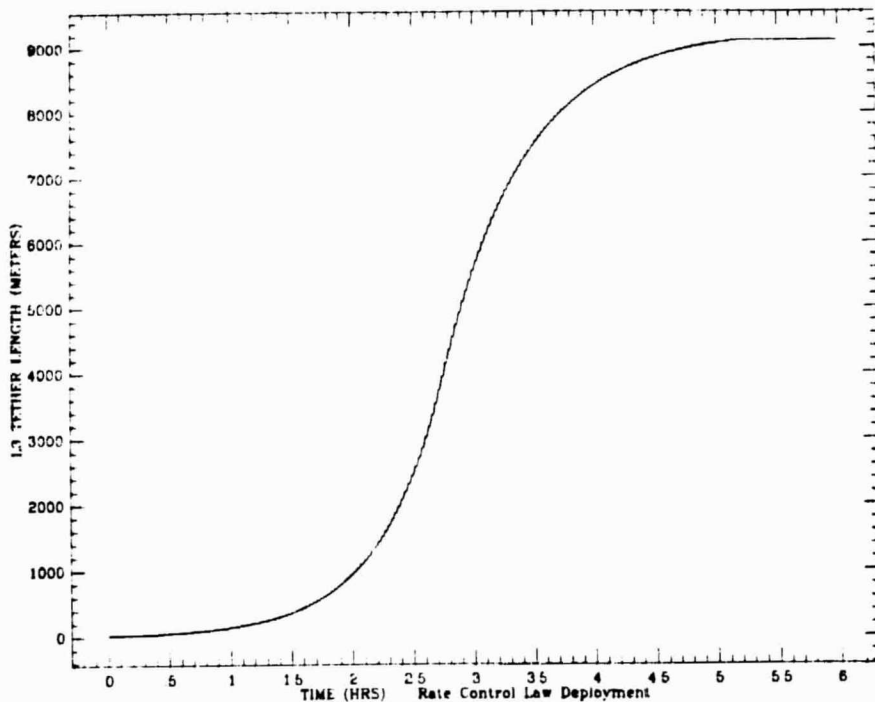
Numerous simulation runs have been performed after implementing the previously described control law in the new simulation program. Different values of parameters, such as α , l_T , σ and l_{SK} have been tested to obtain a set of parameters that results in a well behaved deployment with a low level of acceleration of the middle platform.

The dimensions and the masses used in these simulation runs are equal to the values used in the final report of Phase I. Namely they are: $m_1 = 90600$. kg, $m_2 = 4530$ kg, $m_3 = 9060$. kg, $l_{SK1} = 909.09$ m, $l_{SK3} = 9090.9$ m, orbital altitude = 500 km. Notice that this mathematical model does not separate the orbital center from the center of mass since the gravity field is approximated to the second order. This does not detract from the model since during deployment the major perturbations on m_2 are due to the coupling of the lateral deflection with the libration and since this coupling is not substantially affected by the third order term of the gravity field. The third order terms of the gravity field affect the vertical acceleration components so that a mass located at the system center of mass will actually experience a vertical acceleration different from zero. The conclusion is that the results of these simulation runs are accurate for the horizontal acceleration component (the most important during deployment) while the vertical component does not show the bias dependent on the offset between the center of mass and the orbital center.

The best set of control parameters came out to be: $l_{T1} = 400. \text{ m}$, $l_{T2} = 4000. \text{ m}$, $\sigma_1 = 15 \text{ m}$, $\sigma_2 = 150 \text{ m}$, $1/\alpha = 1874.14 \text{ sec}$ (that implies $\theta_c = 20^\circ$). The deployment was completed in 5.1 hours while the simulation was stopped at 6 hours in order to plot part of a station-keeping (with no tether control). Two sets of figures follow that show results of a successful (and improvable) deployment maneuver. Figure (2.4.1 a,b) and Figure (2.4.2 a,b) show the tether length and tether speed for tether No. 1 and No. 2 respectively (tether No. 2 is called L3 to homogenize the notation in the equations of motion). Notice that these quantities, as mentioned before, are in the ratio l_{SK1}/l_{SK2} and notice also the small discontinuity of the tether speed at the end of the deployment due to the cut off of the exponential deceleration phase. The deployment is initialized with $l_{I1} = 2 \text{ m}$ and $l_{I3} = 20 \text{ m}$. This condition can be actually realized with two deployment booms which are extended at the beginning of the maneuver. These initial tether lengths affect the duration of the maneuver by expediting the initial phase of the deployment. Figure (2.4.3) shows the in-plane angle θ of the constellation vs. time. Because of the choice of the Lagrangian coordinates (see Figure 2.2.1) Figure (2.4.3) must be read together with Figure (2.4.4), which plots the lateral deflection of the middle mass. The constellation's initial attitude is 20° consistent with the selected steady state inclination angle during the first phase of deployment. For this reason the in-plane angle is constant throughout the entire acceleration phase and decreases to the final, residual oscillation amplitude during the deceleration phase. The residual oscillation can be reduced to the steady-state value forced by the J_2 , as shown in the final report of Phase I studies, by means of a tether controlled station-keeping phase. It could also be reduced during the deployment deceleration phase by using a tension control law. This second level improvement will be investigated in the next reporting period if desired by NASA.

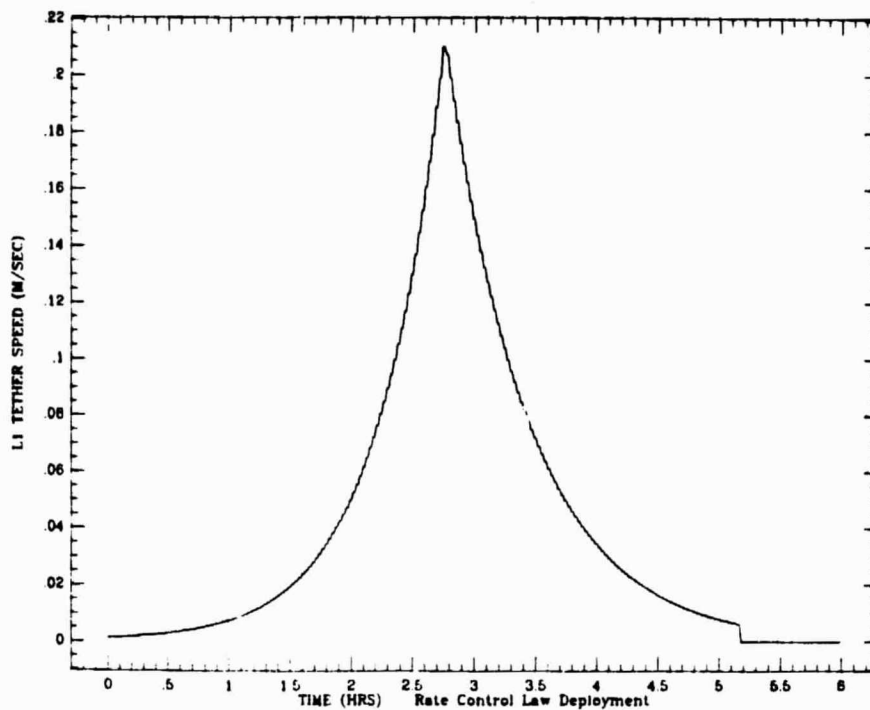


(a) Lower Mass m_1

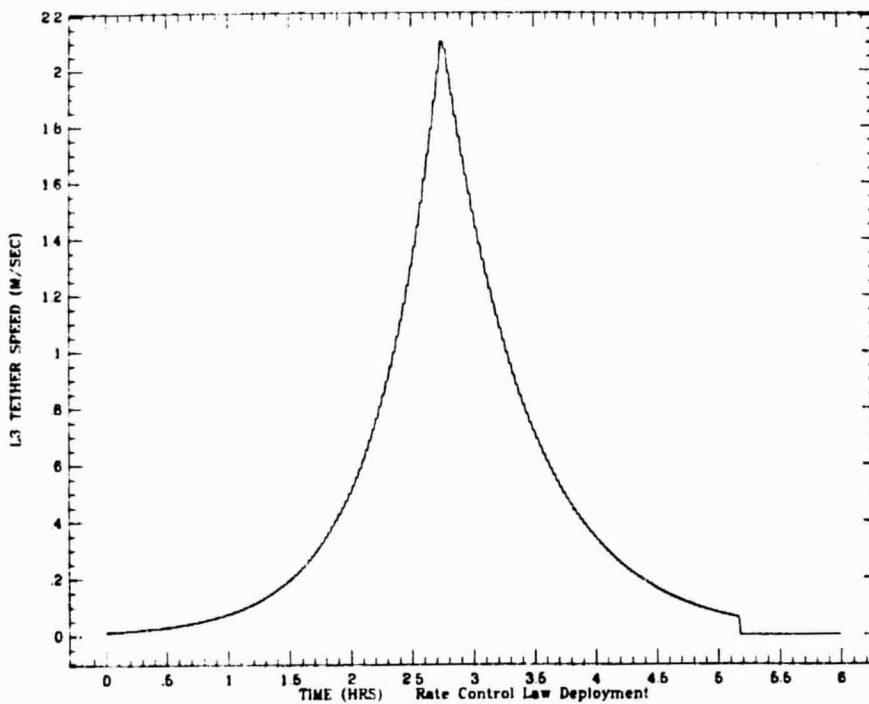


(b) Upper Mass m_3

Figure 2.4.1 Tether length vs. time.



(a) Lower Mass m_1



(b) Upper Mass m_3

Figure 2.4.2 Tether speed vs. time.

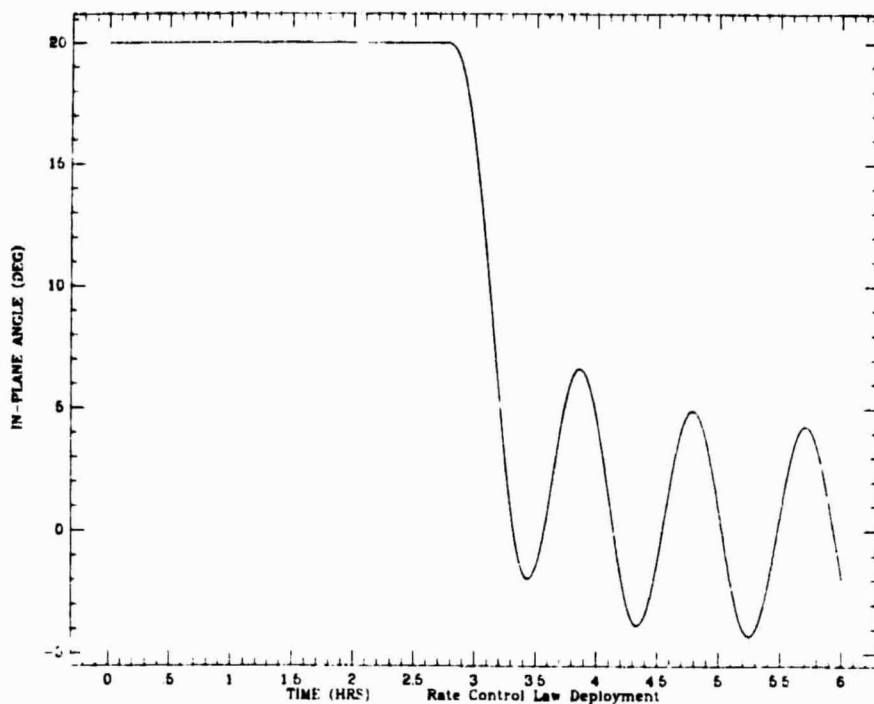


Figure 2.4.3 Constellation's in-plane angle vs. time.
Initial value = 20°.

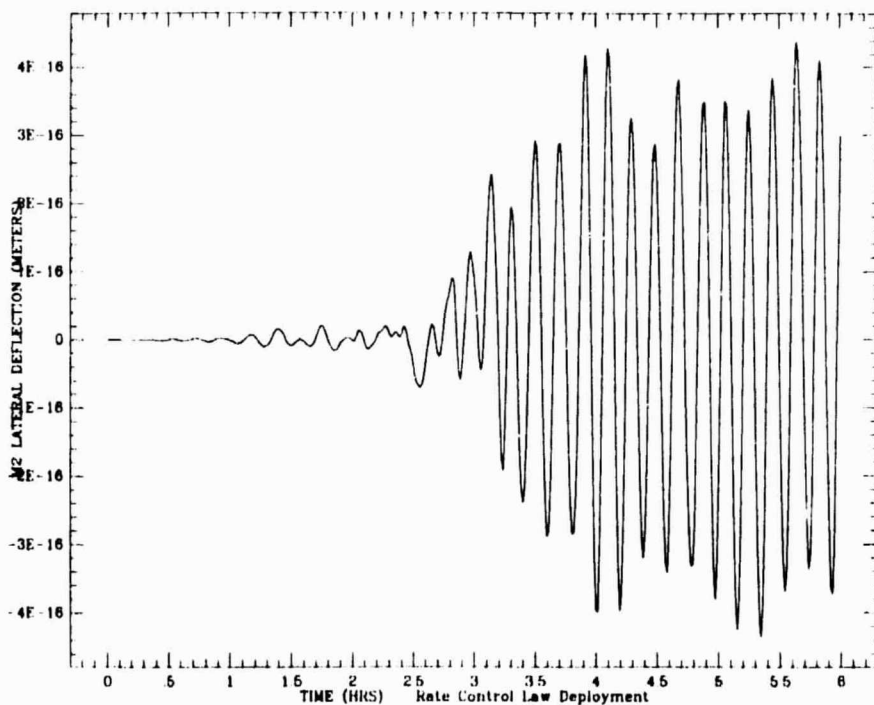
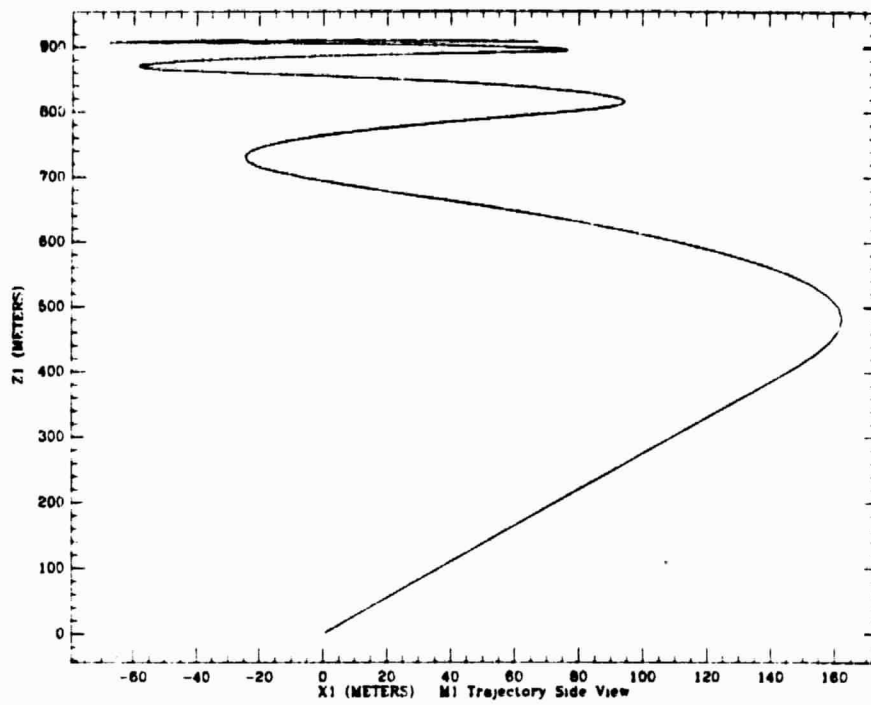


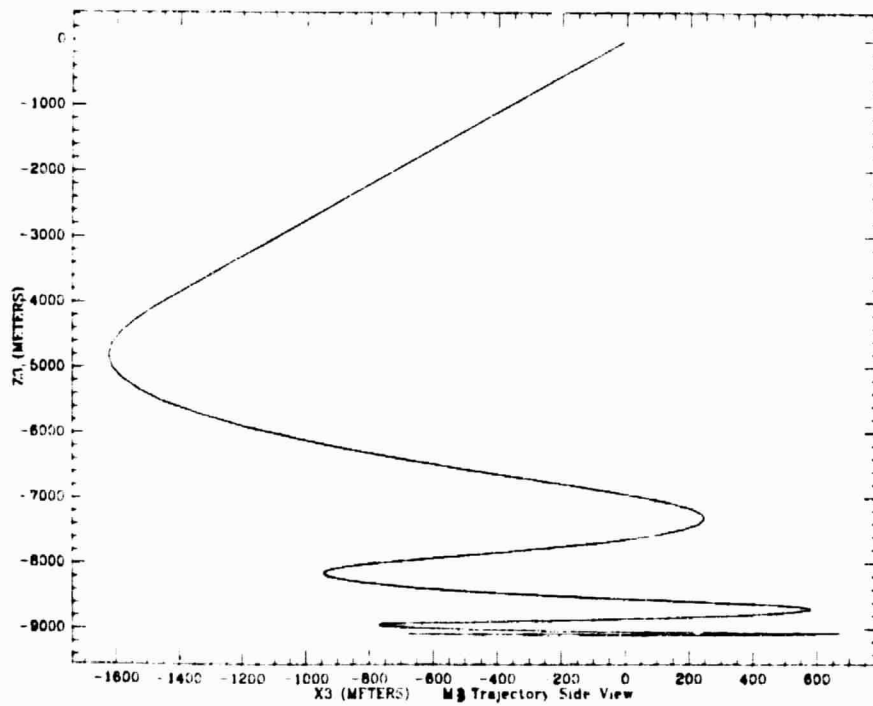
Figure 2.4.4 Middle mass' lateral deflection vs. time.
Initial value = 0.

Figure (2.4.4) shows that the lateral deflection ϵ of the middle mass stays very small if the deployment is initialized with zero lateral deflection. This is because the coupling between lateral oscillation and libration is very weak when the middle platform is located at the system c.m. as mentioned before. Any other location of mass m_2 creates larger lateral deflection and consequently a higher acceleration level. Figure (2.4.5 a,b) show the respective trajectory of the lower and upper mass. Negative numbers mean trajectory outwards from the earth. Figure (2.4.6) shows the tension in tether 1 which is almost exactly equal to the one in tether 2. Figure (2.4.7) is the horizontal component of the acceleration of mass m_2 . The horizontal acceleration component is smaller than the accuracy of our computer in double precision (the middle mass initial lateral deflection is equal to zero) and for this reason it must be considered only as an order of magnitude. Vertical acceleration components and acceleration modulus are not shown here because they are comparable to the horizontal component. Notice also that the vertical component has no bias due to the center of mass-orbital center offset as mentioned before.

It is also interesting to see what the dynamic response and the acceleration level would be if the system starts the deployment with a small alignment error. Some simulation runs were, therefore, performed starting the deployment with different lateral deflections of the system. Results from a simulation run with an initial lateral deflection $\epsilon = 0.05$ m (2 inches) are shown in the following figures. The oscillation amplitude of the lateral deflection stays approximately the same throughout the entire simulation as shown in Figure (2.4.8). The damping of this type of oscillation deserves further study. Damping terms were not included in the control law this time and it would be inter-



(a) Lower Mass m_1



(b) Upper Mass m_3

Figure 2.4.5 Trajectory's side view of the lower and upper mass

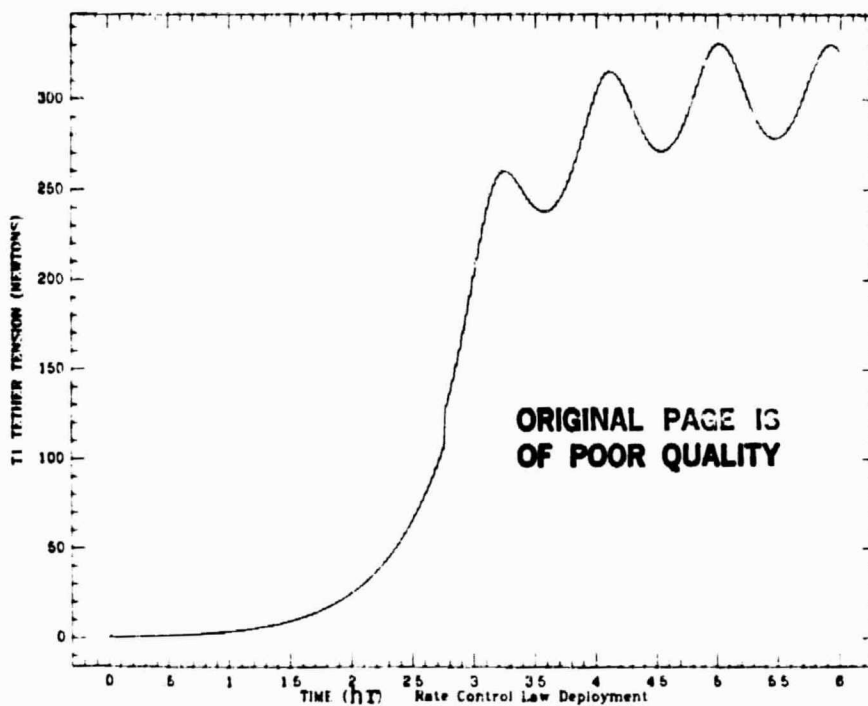


Figure 2.4.6 Tension in tether #1 vs. time.

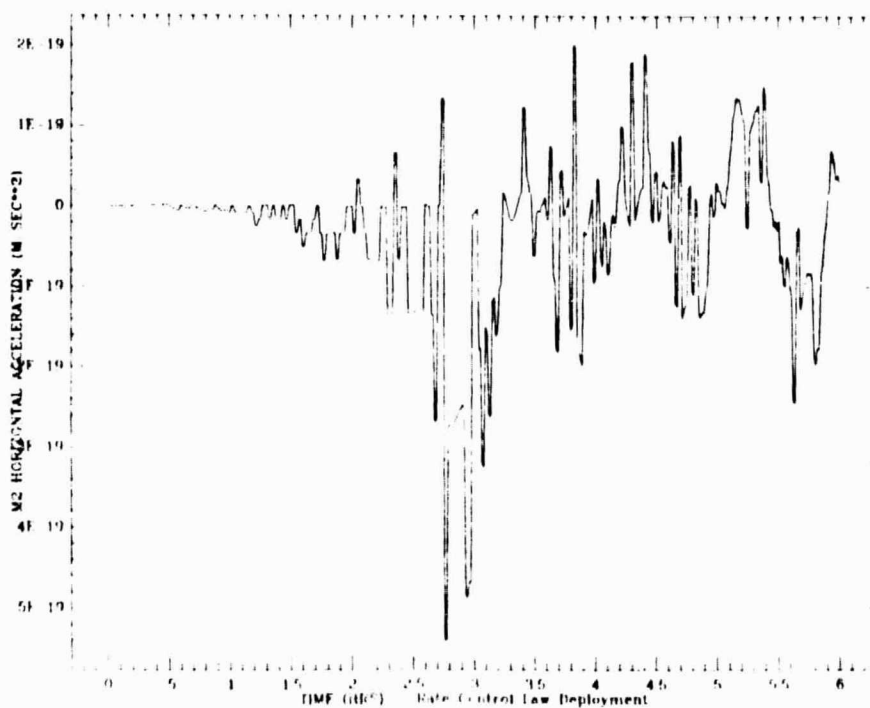


Figure 2.4.7 Horizontal acceleration component of the middle mass vs. time for an initial lateral deflection equal to zero.

esting to see how effective a tension control law could be in damping this oscillation out. Figures (2.4.9), (2.4.10) and (2.4.11) show the horizontal component, vertical component and modulus of the acceleration on the middle mass. All of them are of the order of 10^{-6} m/sec² (10^{-7} g) but these values are strictly dependent on the initial lateral deflection and in any case they should be fine-tuned (and possibly improved) with the use of a tension control law.

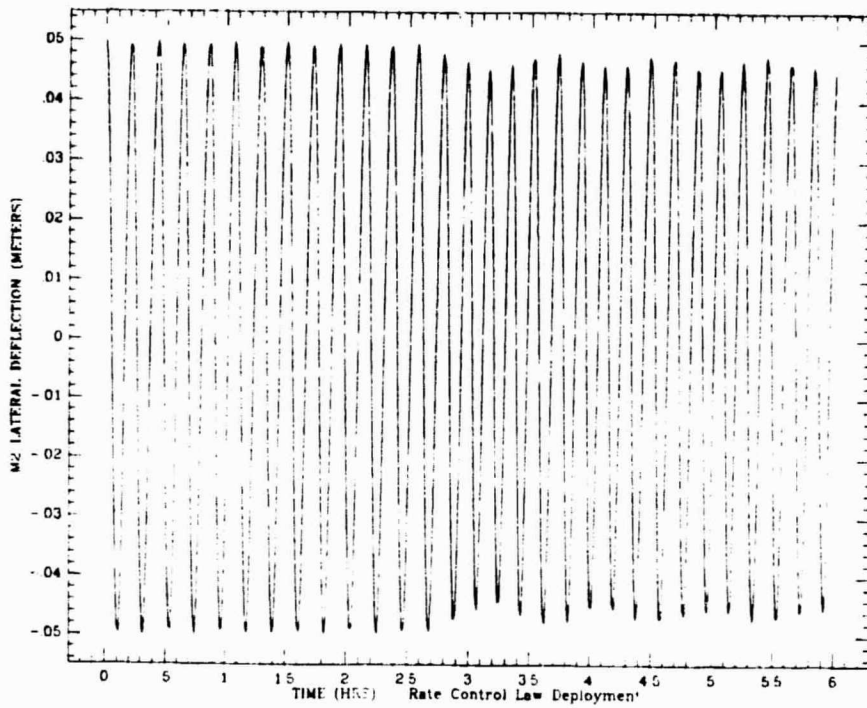


Figure 2.4.8 Lateral deflection of the middle mass vs. time.
Initial value = 0.05 m.

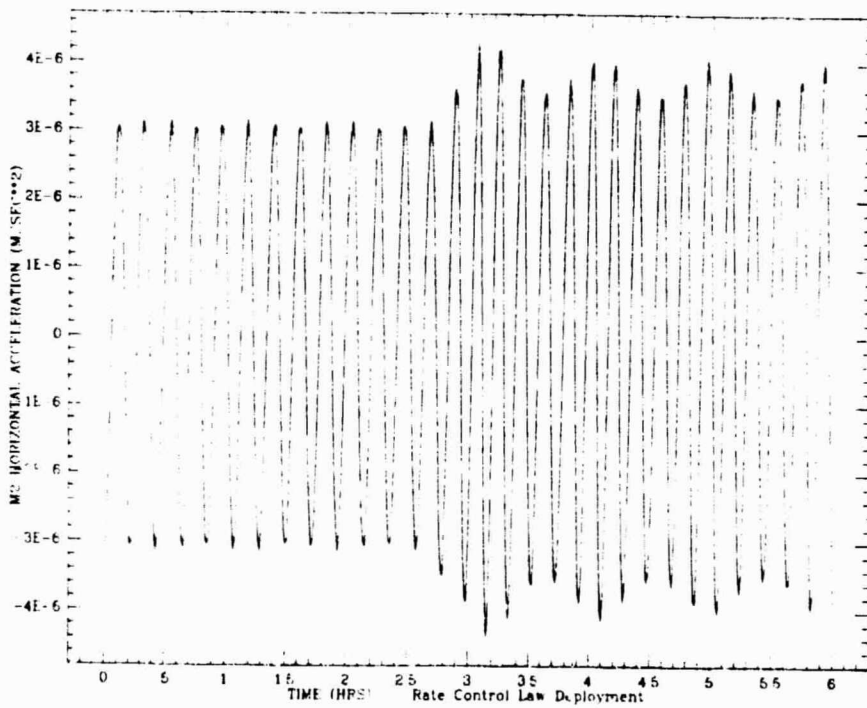


Figure 2.4.9 Horizontal acceleration component of the middle
mass vs. time for an initial lateral deflection = 0.05 m.

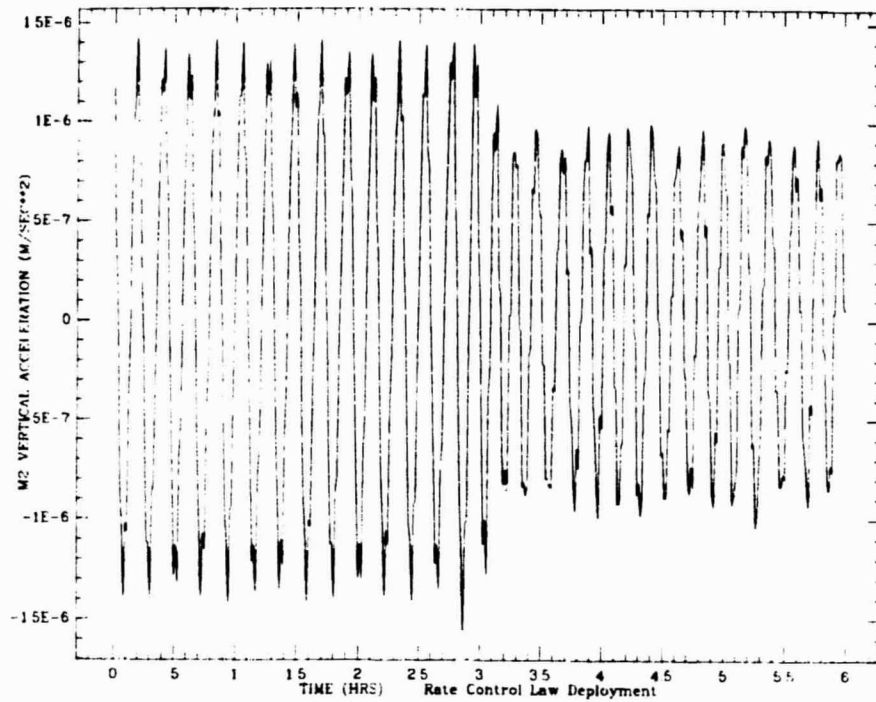


Figure 2.4.10 Vertical acceleration component of the middle mass vs. time for an initial lateral deflection = 0.05 m.

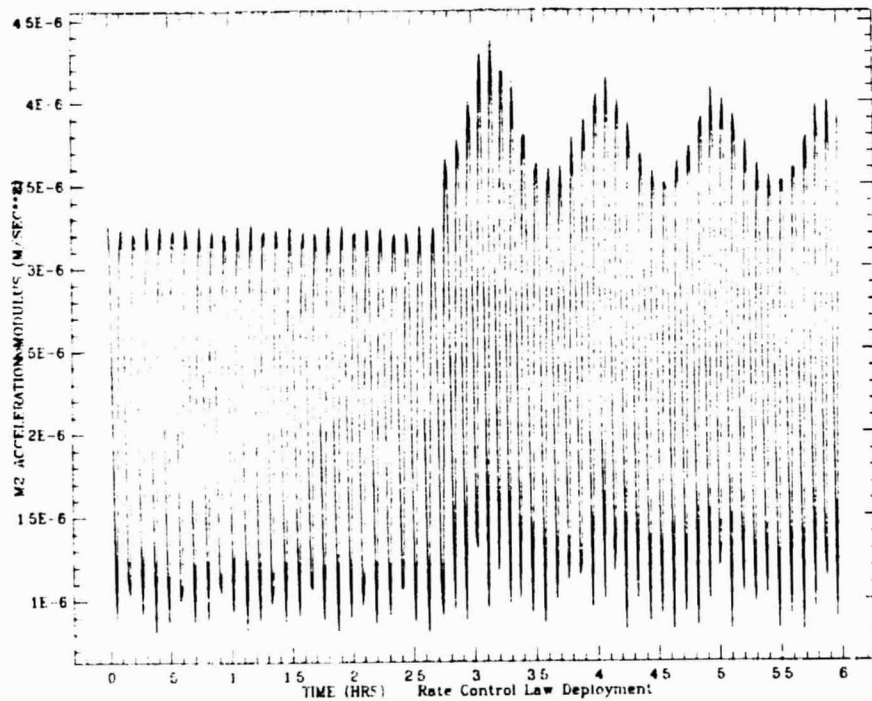


Figure 2.4.11 Acceleration modulus of the middle mass vs. time for an initial lateral deflection = 0.05 m.

2.4.3 Concluding Remarks -

The simple rate control law derived in this study proved to be effective in deploying a single-axis constellation with three masses. By using the same time constant for tether 1 and tether 2 and simultaneous transitions from one phase to another, the middle mass m_2 can be maintained at the center of mass of the system. This strategy reduces the acceleration level induced on the middle platform during deployment. When the deployment is over, the low-g platform can be moved to the orbital center of the system in order to reduce the vertical component of the acceleration. In the system under investigation in this Quarterly Report the orbital center is only 1.2 m lower than the center of mass. It is also important to minimize the initial lateral deflection of mass m_2 with respect to the line through m_1 and m_3 in order to achieve a low acceleration level.

Tension control laws should be investigated to reduce further the final libration and most of all to understand how effective these control laws are in abating the lateral oscillation of the system.

3.0 PROBLEMS ENCOUNTERED DURING REPORTING PERIOD.

None.

4.0 ACTIVITY PLANNED FOR THE NEXT REPORTING PERIOD

During the next reporting period the analysis of the deployment phase of a single-axis constellation with three masses will be further developed. Tension control laws will be investigated. The effect of elastic tethers will be also considered. The tether control law that proves itself most effective for deployment will be verified by SKYHOOK or by a similar high fidelity model specialized to simulate the dynamics of three-mass constellations.

In addition to the above, the dynamics of the constellation when the middle mass travels along the tether in between the two end masses will be studied with the mathematical model derived during this reporting period. This model is perfectly suitable for investigating the situation where the middle platform travels along the tether.